

# Restricted Element-Wise Projection for the Finite Element Method

P. Zajac\*

February 4, 2014

## Abstract

In this work, we propose a projection operator based on restricted element-wise projections, which can be applied to a large set of finite element spaces. In contrast to most other projectors, such as the standard interpolation operator or the well-known Clément's operator, our projection operator does not utilise the node functionals defining the basis functions of the finite element space. Moreover, our operator can be implemented as a modified version of a standard assembly method, thus making it a 'black-box' algorithm, which does not require more information about a finite element space than is already needed for the assembly of a PDE discretisation. Important applications for our operator are its usage as a prolongation and restriction operator for geometric multigrid methods as well as pre- and post-processing like visualisation. We provide local and global  $\mathcal{L}^2$ -error estimates along with numerical experiments verifying the theoretical results.

**Keywords:** finite elements, projections, interpolation, approximation, geometric multigrid

**2010 Mathematics Subject Classifications:** 65D15, 65N15, 65N30, 65N55

## 1 Introduction

Projections of analytical functions into finite element spaces play an important role in both the theory and the practical implementation of the finite element method. In theory, projections – and especially the standard interpolation operator – are used as 'polynomial-preserving operators' for the a-priori error analysis. In conjunction with the Bramble-Hilbert-Lemma, one obtains asymptotical error bounds against powers of the mesh width, thus ensuring the convergence of the finite element method.

From the practical point of view, projections are often required as 'auxiliary' components in a larger context. The first notable application is the projection between two finite element spaces defined on different meshes – primarily for use in geometric multigrid methods. The second important application is pre- and post-processing, where one either needs to project an analytical or discrete function into the finite element space being used for solving a particular PDE or to write the resulting discrete output into a file, which is later on used for e.g. visualisation.

In addition to the standard interpolation, several other projection operators have been proposed in the literature. The most famous example is the 'locally regularised' interpolation proposed by Clément in [5], which performs a local  $\mathcal{L}^2$ -projection into the space of polynomials (of appropriate degree) over a patch of a finite element basis function in the first step, and later on interpolates this polynomial locally. The advantage of this operator is that it can be applied for any  $\mathcal{L}^1$  function, whereas its major practical disadvantage is the necessity of performing a  $\mathcal{L}^2$ -projection over a whole patch. Another drawback is that (e.g. in the case of *iso-parametric* finite element spaces) Clément's operator in general is not a projection.

In [15], Schieweck presented a projection operator based on restricted element-wise interpolation. In contrast to the standard interpolation operator, his approach requires the function to

---

\*Institut für Angewandte Mathematik und Numerik, Technische Universität Dortmund, Vogelpothsweg 87, D-44227 Dortmund, Germany

be projected to be smooth only element-wise, thus making it a suitable candidate for multigrid prolongation operators for nonconforming finite elements such as e.g. the Crouzeix-Raviart or Rannacher-Turek elements, see [8] and [9]. Furthermore, the author also proposes a regularised version, which can be applied to project any  $\mathcal{L}^1$  function.

However, the two previously mentioned projection operators require the application of the finite element *node functionals* to the function to be projected, which is a severe drawback when it comes to implementing the operator in a software package. Although this is simple enough for Lagrange-type finite elements, the node functionals may require far more information and effort than only evaluation in a set of points. One example are Hermite or Argyris elements used for higher-order PDEs, see e.g. [1], where the application of the node functionals onto the function to be projected requires computation of the function's partial derivatives, which, however, may not be available. Furthermore, there exist finite element spaces whose basis functions are constructed in a more 'exotic' way, e.g. by a local optimisation approach as in [14].

Another projection approach was proposed by Scott and Zhang in [13]. Their projection operator performs local projections on either an element or a facet, depending on the type of the node functional of a basis function. Although this operator is shown to be a boundary-condition-preserving projection, it has only been defined for Lagrange elements. Moreover, the projection over facets requires the function to be projected to have sufficient smoothness to ensure that its trace over any facet is well-defined. In consequence, this rules out its application for nonconforming finite elements.

Finally, one also has the possibility of performing a 'real'  $\mathcal{L}^2$ -projection into the finite element space. Although this projection is easy to implement and applicable for any finite element space, it requires to solve a (usually large) linear system with the mass matrix – which is unproblematic if only a handful of projections are to be performed. However, especially in the context of geometric multigrid methods, the  $\mathcal{L}^2$ -projection is not a candidate for prolongation operators due to its frequent application and relatively high computational cost, unless one applies some sort of *lumping* to the mass matrix, which may not be possible for all finite element spaces.

These practical drawbacks serve as motivation for our new projection operator, whose primary design goals are:

- In the special case of projections between two finite element spaces, it shall be possible to assemble the projection operator into a sparse matrix efficiently, thus allowing its application to be reduced to a sparse matrix-vector multiplication.
- The implementation of the projection shall only utilise software components which are already required for the assembly of a mass matrix and a right hand side vector.
- The projection shall be applicable for a large set of finite element spaces, especially nonconforming and higher order ones.
- The domain (of definition) of the projection shall contain the set of all  $\mathcal{L}^2(\Omega)$  functions.
- The projection error shall be uniformly bounded by the discretisation error.
- The projection shall have a 'local' character in the sense that the projection  $u_h$  of a function  $u$  restricted onto a single element  $T$  shall only depend on  $u$  restricted onto a vicinity of  $T$ .

In this work, we present a new projection operator, which fulfills all these requirements. Its construction is related to the one proposed by Schieweck in [15], whereas we perform element-wise  $\mathcal{L}^2$ -projections instead of element-wise interpolations. As the motivations for our projection operator are primarily of practical nature, we estimate the projection error against the discretisation error rather than against powers of the mesh width in our theoretical a-priori error analysis. The discretisation error itself can then be estimated using other interpolation operators, such as the one proposed by Clément, which is a fundamental part of every a-priori finite element space analysis.

Our theoretical analysis will yield a set of abstract assumptions, which we later on verify for parametric finite element spaces on shape-regular conforming meshes, thus proving that our projection operator is applicable for a significantly large set of finite element spaces.

We also discuss the practical aspects of our projection operator and show how it can be implemented efficiently as a modified matrix and right-hand-side assembly algorithm, utilising only standard finite element software functionality. Finally, we present a set of numerical examples, which practically verify our theoretical results.

## 2 Basic Definitions and Notations

For  $n \in \mathbb{N}$ , let  $\Omega \subset \mathbb{R}^n$  denote a bounded open domain with a Lipschitz boundary  $\partial\Omega$ . For any non-empty subset  $T \subset \Omega$ , we denote by  $\text{vol}(T) := \int_T 1$  the volume of  $T$ , and for any  $u, v \in \mathcal{L}^2(T)$ , we denote by  $\langle u, v \rangle_{0,T}$  the  $\mathcal{L}^2$  scalar product over  $T$  and by  $\|u\|_{0,T}$  the  $\mathcal{L}^2$  norm of  $u$  over  $T$ . By  $T_h$  we denote a mesh discretising the domain  $\Omega \subset \mathbb{R}^n$ , i.e. a finite decomposition of  $\Omega$  into elements  $T \in T_h$  in the sense of Ciarlet, see [1]. For any set of elements  $\delta \subseteq T_h$  we use the short notations

$$\|u\|_{0,\delta} := \left( \sum_{T \in \delta} \|u\|_{0,T}^2 \right)^{\frac{1}{2}}, \quad \text{vol}(\delta) := \sum_{T \in \delta} \text{vol}(T).$$

Let  $V_h \subset \mathcal{L}^2(\Omega)$  denote a finite element space defined on  $T_h$  and let  $B_h = \{\varphi_1, \dots, \varphi_m\}$  denote the basis of  $V_h$ . Then for any  $T \in T_h$  we denote by

$$\mathcal{I}(T) := \{ i \in \{1, \dots, m\} \mid \text{supp}(\varphi_i) \cap T \neq \emptyset \} \quad (1)$$

the *dof-set of  $T$* , i.e., the set of all indices of basis functions  $\varphi_i$ , whose supports intersect with the element  $T$ , and its counterpart, the *patch of  $i$* , by

$$\sigma(i) := \{ T \in T_h \mid i \in \mathcal{I}(T) \}. \quad (2)$$

Furthermore, we denote by

$$\delta(T) := \{ T' \in \sigma(i) \mid i \in \mathcal{I}(T) \} \quad (3)$$

the *dof-vicinity of  $T$* , i.e. the set of all elements  $T' \in T_h$ , which share at least one common basis function  $\varphi_i$  of  $V_h$  with  $T$ . We define the corresponding discontinuous space of  $V_h$  by

$$\tilde{V}_h := \{ \tilde{v}_h \in \mathcal{L}^2(\Omega) \mid \forall T \in T_h : \tilde{v}_h|_T \in V_h|_T \}, \quad (4)$$

where for any  $T \in T_h$  we have

$$V_h|_T := \{ v_h|_T \in \mathcal{L}^2(T) \mid v_h \in V_h \}.$$

For any  $T \in T_h$  and any  $i \in \mathcal{I}(T)$  we define

$$\tilde{\varphi}_{T,i}(x) := \begin{cases} \varphi_i(x), & \text{for } x \in T \\ 0, & \text{otherwise.} \end{cases} \quad (5)$$

## 3 The Projection Operator

Throughout this section, we consider a set of basis functions  $B_h$  spanning a finite element space  $V_h$  on a mesh  $T_h$  discretising a domain  $\Omega \subset \mathbb{R}^n$ . Before we begin with the construction of our projection operator, we first need to make an assumption on the basis  $B_h$  that will be crucial for this work: We shall assume that

$$\forall T \in T_h : \quad \text{card}(\mathcal{I}(T)) = \dim(V_h|_T), \quad (\mathbf{BA})$$

i.e., the number of basis functions which do not vanish on an element  $T \in T_h$  shall be equal to the dimension of the space that these basis functions span on the element  $T$ . This assumption is not restrictive, as it is fulfilled for the vast majority of all nodal finite element spaces. Under this assumption, we directly see that the set of all  $\tilde{\varphi}_{T,i}$  as defined in (5) forms a basis spanning  $\tilde{V}_h$  and this allows us to represent any  $\tilde{v}_h \in \tilde{V}_h$  by its corresponding unique coefficients  $\tilde{v}_{T,i} \in \mathbb{R}$  for  $T \in T_h$  and  $i \in \mathcal{I}(T)$  by

$$\tilde{v}_h = \sum_{T \in T_h} \sum_{i \in \mathcal{I}(T)} \tilde{v}_{T,i} \cdot \tilde{\varphi}_{T,i}. \quad (6)$$

### The discontinuous $\mathcal{L}^2$ -projection operator $\tilde{P}_h$

We denote by  $\tilde{P}_h : \mathcal{L}^2(\Omega) \rightarrow \tilde{V}_h$  the  $\mathcal{L}^2$ -projection into  $\tilde{V}_h$ , i.e. for any  $u \in \mathcal{L}^2(\Omega)$  it shall hold

$$\forall \tilde{v}_h \in \tilde{V}_h : \quad \langle u - \tilde{P}_h(u), \tilde{v}_h \rangle_{0,\Omega} = 0, \quad (7)$$

and, as  $\tilde{V}_h$  is discontinuous, we have that (7) is equivalent to

$$\forall T \in T_h, \forall \tilde{v}_h \in \tilde{V}_h : \quad \langle u - \tilde{P}_h(u), \tilde{v}_h \rangle_{0,T} = 0. \quad (8)$$

It is well known that for any  $u \in \mathcal{L}^2(\Omega)$  the coefficients  $\tilde{u}_{T,i} \in \mathbb{R}$  of the projection

$$\sum_{T \in T_h} \sum_{i \in \mathcal{I}(T)} \tilde{u}_{T,i} \cdot \tilde{\varphi}_{T,i} = \tilde{u}_h := \tilde{P}_h(u) \quad (9)$$

are given by the solution of the linear systems

$$M_T \cdot \tilde{u}_T = u_T^* \quad (10)$$

for any  $T \in T_h$ , where for  $(j_1, \dots, j_l) := \mathcal{I}(T)$  we have

$$(M_T)_{k,i} := \langle \tilde{\varphi}_{T,j_i}, \tilde{\varphi}_{T,j_k} \rangle_{0,T} \quad (\tilde{u}_T)_i = \tilde{u}_{T,j_i}, \quad (u_T^*)_k := \langle u, \tilde{\varphi}_{T,j_k} \rangle_{0,T}. \quad (11)$$

At this point, we have to investigate the local mass matrix  $M_T$  in (10): The size of the matrix equals the cardinality of  $\mathcal{I}(T)$ , whereas its rank is equal to the dimension of  $\tilde{V}_h|_T = V_h|_T$ . Now, under the assumption **(BA)** those two quantities coincide, and therefore the local mass matrix  $M_T$  is regular for any  $T \in T_h$ .

### The primal restriction operator $R_h^\omega$

We now define the primal restriction operator  $R_h^\omega : \tilde{V}_h \rightarrow V_h$ , such that it maps any  $\tilde{u}_h \in \tilde{V}_h$  represented by its unique coefficients  $\tilde{u}_{T,i}$ ,

$$R_h^\omega(\tilde{u}_h) := \sum_{i=1}^m \left( \sum_{T \in \sigma(i)} \omega_{T,i} \cdot \tilde{u}_{T,i} \right) \cdot \varphi_i, \quad (12)$$

where the coefficients  $\omega_{T,i} \in \mathbb{R}$  are user-chosen weights describing a convex combination of all  $\tilde{u}_{T,i}$  for any  $i$ , i.e., it shall hold that for all  $i \in \{1, \dots, m\}$ :

$$\forall T \in \sigma(i) : 0 \leq \omega_{T,i} \leq 1 \quad \text{and} \quad \sum_{T \in \sigma(i)} \omega_{T,i} = 1. \quad (13)$$

There are various possible choices for the weights: The most simple choice is to set

$$\omega_{T,i} := \frac{1}{\text{card}(\sigma(i))}, \quad (14)$$

which leads to the *arithmetic average* of all local contributions. Another example, which we will consider in the numerical experiments later, is the *volume-weighted average*

$$\omega_{T,i} := \frac{\text{vol}(T)}{\text{vol}(\sigma(i))}. \quad (15)$$

### The projection operator $P_h^\omega$

With our primal restriction operator  $R_h^\omega$  and the previously defined discontinuous  $\mathcal{L}^2$ -projection operator  $\tilde{P}_h$ , we can now formally define our projection operator  $P_h^\omega$  as a composition thereof:

$$P_h^\omega := R_h^\omega \circ \tilde{P}_h : \mathcal{L}^2(\Omega) \rightarrow V_h. \quad (16)$$

As a first result, the following lemma will show that the operator  $P_h^\omega$  is in fact a projection, which will be an important property for the proofs of the a-priori error estimates.

**Lemma 1**

The operators  $R_h^\omega$  and  $P_h^\omega$  defined in (12) and (16), respectively, are projections, i.e. for any  $v_h \in V_h \subset \mathcal{L}^2(\Omega)$  it holds

$$R_h^\omega(v_h) = P_h^\omega(v_h) = v_h. \quad (17)$$

*Proof.* Let  $v_h \in V_h$  be arbitrary, let  $m := \dim(V_h)$  and let  $v_i \in \mathbb{R}$  denote the coefficients of  $v_h$ . By construction of the basis of  $\tilde{V}_h$  in (5), by (6) we have that

$$\forall i \in \{1, \dots, m\}, \forall T \in \sigma(i) : v_i = \tilde{v}_{T,i}. \quad (*)$$

Now let  $v'_h := R_h^\omega(v_h)$ , then for the coefficients  $v'_i \in \mathbb{R}$  of  $v'_h$  we have for any  $i \in \{1, \dots, m\}$

$$v'_i \stackrel{(12)}{=} \sum_{T \in \sigma(i)} \omega_{T,i} \cdot \tilde{v}_{T,i} \stackrel{(*)}{=} \sum_{T \in \sigma(i)} \omega_{T,i} \cdot v_i \stackrel{(13)}{=} v_i,$$

and therefore  $R_h^\omega(v_h) = v_h$ . Furthermore, as  $\tilde{P}_h : \mathcal{L}^2(\Omega) \rightarrow \tilde{V}_h$  is a projection by definition, it also holds for any  $v_h \in V_h$  that

$$P_h^\omega(v_h) = R_h^\omega \circ \tilde{P}_h(v_h) = R_h^\omega(v_h) = v_h. \quad \blacksquare$$

**Correlation to the interpolation operator**

Our projection operator  $P_h^\omega$  requires the solution of local linear systems  $M_T \cdot \tilde{u}_T = u_T^*$  as given in (11). The assembly of the mass matrix  $M_T$  and the local right-hand-side vector  $u_T^*$  requires integration over the corresponding element  $T \in T_h$ , and in practice these integrals are approximated by cubature formulas. In consequence, the choice of the cubature formula has an impact on our projection operator  $P_h^\omega$ , i.e., two different cubature formulas will in general yield two different projection operators, unless the order of the cubature formula is high enough such that the integration error is negligible.

In the case of Lagrange elements, i.e., when the basis  $B_h$  is associated with a set of nodal points, see e.g. [1], one may choose a *lumped* cubature formula, i.e., a cubature rule whose cubature points coincide with the nodal points of the basis  $B_h$ . In this case, the local mass matrix  $M_T$  becomes diagonal, and one can easily show that for any choice of restriction weights  $\omega_{T,i}$  the projection operator  $P_h^\omega$  coincides with the interpolation operator of  $V_h$ , which is usually denoted as  $\Pi_h$ . As an example one may consider the standard  $P_1$  or  $Q_1$  space, whose basis functions are associated with the function values in the vertices of the mesh  $T_h$ , in combination with the trapezoidal cubature rule.

**4 A-priori Estimates**

In this section, we want to deduce a-priori stability and error estimates for the projection operator  $P_h^\omega$ . In contrast to most estimation techniques, we will not directly bound the error against powers of the mesh width, but we show that the local and global  $\mathcal{L}^2$ -errors are bounded by the discretisation error of the corresponding finite element space  $V_h$  instead. This approach has two advantages: First, we will require few abstract assumptions on the underlying finite element space, thus allowing us to provide estimates without using the actual definition of  $V_h$ , and, second, the discretisation error is a quantity that is usually estimated by powers of the mesh width (and possibly other quantities such as e.g. the element aspect ratio) as part of the standard analysis of a finite element space.

**4.1  $\mathcal{L}^2$ -Stability Estimates**

As our projection operator is in general not an orthogonal projection with respect to the  $\mathcal{L}^2$  scalar product, we will first prove a local stability estimate for the primal restriction operator  $R_h^\omega$ , which is a key ingredient for the error estimates. The following theorem summarises all requirements on the finite element space that are necessary for the stability estimate.

**Theorem 2:** Local  $\mathcal{L}^2$ -Stability of  $R_h^\omega$

Let  $V_h$  denote a finite element space defined on a mesh  $T_h$ , whose basis  $B_h$  fulfills the assumption **(BA)**, and assume there exists a uniform constant  $c_1 > 0$ , such that for any  $T \in T_h$  there exists a  $\tau_T > 0$ , such that the norm equivalence

$$c_1^{-1} \cdot \tau_T \cdot \|\tilde{v}_h\|_{0,T} \leq \|\tilde{v}_h\|_{0,T} \leq c_1 \cdot \tau_T \cdot \|\tilde{v}_h\|_{0,T} \quad (\mathbf{A1})$$

holds for any  $T \in T_h$  and any  $\tilde{v}_h \in \tilde{V}_h$ , where

$$\|\tilde{v}_h\|_{0,T} := \left( \sum_{i \in \mathcal{I}(T)} |\tilde{v}_{T,i}|^2 \right)^{\frac{1}{2}} \quad (18)$$

denotes the euclidean norm of all coefficients  $\tilde{v}_{T,i}$  contained in the dof-set of  $T$ . Furthermore, assume there exists a second uniform constant  $c_2 > 0$ , such that for any  $T \in T_h$  and any  $T' \in \delta(T)$  it holds that

$$\tau_T \leq c_2 \cdot \tau_{T'}. \quad (\mathbf{A2})$$

Then the primal restriction operator  $R_h^\omega : \tilde{V}_h \rightarrow V_h$  fulfills the local stability estimate

$$\|R_h^\omega(\tilde{v}_h)\|_{0,T} \leq c_R \|\tilde{v}_h\|_{0,\delta(T)} \quad (19)$$

for all  $\tilde{v}_h \in \tilde{V}_h$  and all  $T \in T_h$  with  $c_R = c_1^2 c_2$ .

Before we continue with the proof of the theorem, let us first take a closer look at the two new assumptions the theorem introduced. The two assumptions **(A1)** and **(A2)** require that the  $\mathcal{L}^2$ -norm over an element  $T$  is equivalent to the euclidean norm of all basis function coefficients on that element, where we allow an element-dependent parameter  $\tau_T$ , which shall be bounded in the vicinity of  $T$ . Although these assumptions seem unusual, we will see in section 4.3 that these assumptions are not restrictive, as they are fulfilled for all parametric finite elements on shape-regular conforming meshes – which covers the majority of all commonly used finite element spaces. Moreover, note that the theorem does not refer to a particular choice of weights  $\omega_{T',i} \in \mathbb{R}$  for the restriction operator  $R_h^\omega$  – the above estimate holds true for all possible choices of weights that form a convex combination, as we will now see in the following proof.

*Proof of Theorem 2.* Let  $T \in T_h$  and  $\tilde{v}_h \in \tilde{V}_h$  be arbitrary and let  $\tilde{v}_{T,i} \in \mathbb{R}$  denote the coefficients of  $\tilde{v}_h$ , then

$$\|R_h^\omega(\tilde{v}_h)\|_{0,T}^2 \stackrel{(\mathbf{A1})}{\leq} c_1^2 \tau_T^2 \|\tilde{v}_h\|_{0,T}^2 \stackrel{(12)}{=} c_1^2 \tau_T^2 \sum_{i \in \mathcal{I}(T)} \left| \sum_{T' \in \sigma(i)} \omega_{T',i} \tilde{v}_{T',i} \right|^2,$$

and application of the Cauchy-Schwarz inequality to the inner sum yields

$$\|R_h^\omega(\tilde{v}_h)\|_{0,T}^2 \leq c_1^2 \tau_T^2 \sum_{i \in \mathcal{I}(T)} \left( \sum_{T' \in \sigma(i)} |\omega_{T',i}|^2 \right) \cdot \left( \sum_{T' \in \sigma(i)} |\tilde{v}_{T',i}|^2 \right). \quad (*)$$

By assumption (13) we have  $0 \leq \omega_{T',i} \leq 1$  and therefore

$$\sum_{T' \in \sigma(i)} |\omega_{T',i}|^2 \leq \sum_{T' \in \sigma(i)} \omega_{T',i} \stackrel{(13)}{=} 1. \quad (**)$$

By combining (\*) and (\*\*) we get

$$\begin{aligned}
\|R_h^\omega(\tilde{v}_h)\|_{0,T}^2 &\leq c_1^2 \tau_T^2 \sum_{i \in \mathcal{I}(T)} \sum_{T' \in \sigma(i)} |\tilde{v}_{T',i}|^2 \\
&\stackrel{(3)}{\leq} c_1^2 \tau_T^2 \sum_{T' \in \delta(T)} \sum_{i \in \mathcal{I}(T')} |\tilde{v}_{T',i}|^2 \\
&\stackrel{(18)}{=} c_1^2 \tau_T^2 \sum_{T' \in \delta(T)} \|\tilde{v}_h\|_{0,T'}^2 \\
&\stackrel{(A1)}{\leq} c_1^4 \tau_T^2 \sum_{T' \in \delta(T)} \tau_{T'}^{-2} \|\tilde{v}_h\|_{0,T'}^2 \\
&\stackrel{(A2)}{\leq} c_1^4 c_2^2 \sum_{T' \in \delta(T)} \|\tilde{v}_h\|_{0,T'}^2 \\
&= c_1^4 c_2^2 \|\tilde{v}_h\|_{0,\delta(T)}^2.
\end{aligned}$$

■

As a direct consequence of the stability of the restriction operator  $R_h^\omega$ , we can also provide a stability estimate for the projection operator  $P_h^\omega$ .

**Corollary 3:** Local  $\mathcal{L}^2$ -Stability of  $P_h^\omega$

Under the assumptions of Theorem 2 it holds for any  $u \in \mathcal{L}^2(\Omega)$ :

$$\|P_h^\omega(u)\|_{0,T} \leq c_R \|u\|_{0,\delta(T)}. \quad (20)$$

*Proof.* Let  $u \in \mathcal{L}^2(\Omega)$  be arbitrary, then for  $\tilde{u}_h := \tilde{P}_h(u)$  we have by (8) that for any  $T \in T_h$

$$\|\tilde{u}_h\|_{0,T} \leq \|u\|_{0,T}, \quad (*)$$

because  $\tilde{P}_h$  is the orthogonal  $\mathcal{L}^2$ -projection into  $\tilde{V}_h$ . By definition we have  $P_h^\omega(u) = R_h^\omega(\tilde{u}_h)$ , so (19) and (\*) imply the assumption. ■

## 4.2 $\mathcal{L}^2$ -Error Estimates

With the stability estimates we have established so far and by the fact that the operator  $P_h^\omega$  is a projection, we can now easily derive a local error estimate, which bounds the  $\mathcal{L}^2$ -error on an element  $T \in T_h$  by the error of the optimal approximation in the vicinity of  $T$ .

**Theorem 4:** Local  $\mathcal{L}^2$ -Error Estimate

Under the assumptions of Theorem 2 the projection operator  $P_h^\omega : \mathcal{L}^2(\Omega) \rightarrow V_h$  fulfills the local estimate

$$\|u - P_h^\omega(u)\|_{0,T} \leq c_P \cdot \inf_{v_h \in V_h} \|u - v_h\|_{0,\delta(T)} \quad (21)$$

for all  $T \in T_h$  and all  $u \in \mathcal{L}^2(\Omega)$  for  $c_P = 1 + 2c_R$ .

*Proof.* Let  $u \in \mathcal{L}^2(\Omega)$ ,  $v_h \in V_h$  and  $T \in T_h$  be arbitrary and let  $\tilde{u}_h := \tilde{P}_h(u) \in \tilde{V}_h$  denote the  $\mathcal{L}^2$ -projection of  $u$  into  $\tilde{V}_h$ , then

$$\begin{aligned}
\|u - P_h^\omega(u)\|_{0,T} &\stackrel{(16)}{=} \|u - v_h + v_h - R_h^\omega(\tilde{u}_h)\|_{0,T} \\
&\stackrel{(17)}{\leq} \|u - v_h\|_{0,T} + \|R_h^\omega(\tilde{u}_h - v_h)\|_{0,T} \\
&\stackrel{(19)}{\leq} \|u - v_h\|_{0,T} + c_R \|\tilde{u}_h - v_h\|_{0,\delta(T)} \\
&\leq \|u - v_h\|_{0,\delta(T)} + c_R \|\tilde{u}_h - u + u - v_h\|_{0,\delta(T)} \\
&\leq (1 + c_R) \cdot \|u - v_h\|_{0,\delta(T)} + c_R \|u - \tilde{u}_h\|_{0,\delta(T)}. \quad (*)
\end{aligned}$$

Now as  $\tilde{u}_h$  is the  $\mathcal{L}^2$ -projection of  $u$  into  $\tilde{V}_h$ , by (8) we have that  $\|u - \tilde{u}_h\|_{0,\delta(T)} \leq \|u - v_h\|_{0,\delta(T)}$  for any  $v_h \in V_h \subseteq \tilde{V}_h$  and with (\*) we finally obtain

$$\|u - P_h^\omega(u)\|_{0,T} \leq (1 + 2c_R) \cdot \|u - v_h\|_{0,\delta(T)}.$$

■

With the local error estimate from the previous theorem, we can prove a global one under one additional assumption, which we shall analyse more closely in the next section.

**Theorem 5:** Global  $\mathcal{L}^2$ -Error Estimate

Let the assumptions of Theorem 4 hold and furthermore assume there exists a uniform constant  $c_3 > 0$ , such that for any  $T \in T_h$  it holds that

$$\text{card}(\delta(T)) \leq c_3, \tag{A3}$$

then the projection operator  $P_h^\omega : \mathcal{L}^2(\Omega) \rightarrow V_h$  fulfills the global estimate

$$\|u - P_h^\omega(u)\|_{0,\Omega} \leq c \cdot \inf_{v_h \in V_h} \|u - v_h\|_{0,\Omega} \tag{22}$$

for all  $u \in \mathcal{L}^2(\Omega)$  with  $c = c_P c_3$ .

*Proof.* Let  $u \in \mathcal{L}^2(\Omega)$  and  $v_h \in V_h$  be arbitrary, then

$$\|u - P_h^\omega(u)\|_{0,\Omega}^2 \stackrel{(21)}{\leq} c_P \sum_{T \in T_h} \|u - v_h\|_{0,\delta(T)}^2 = c_P \sum_{T \in T_h} \sum_{T' \in \delta(T)} \|u - v_h\|_{0,T'}^2, \tag{*}$$

and by (A3) we have that any  $T' \in T_h$  appears at most  $c_3$  times in the double sum, so we obtain

$$\|u - P_h^\omega(u)\|_{0,\Omega}^2 \stackrel{(*)}{\leq} c_P c_3 \sum_{T \in T_h} \|u - v_h\|_{0,T}^2 = c_P c_3 \cdot \|u - v_h\|_{0,\Omega}^2.$$

■

### 4.3 Parametric families on conforming shape-regular meshes

The estimates we have obtained so far introduced three assumptions (A1), (A2) and (A3) in addition to the basis assumption (BA), which was already required to ensure that our projection operator  $P_h^\omega$  is well-defined. In this section, we want to show that all these four assumptions are fulfilled for all parametric finite element spaces on conforming shape-regular meshes, where a mesh  $T_h$  is said to be *conforming* if for any two different elements  $T, T' \in T_h$  the intersection  $T \cap T'$  is either the empty set, a common vertex or a common  $k$ -dimensional face of both elements for some  $0 < k < n$ . Throughout this section, we implicitly assume that the mesh  $T_h$  is conforming.

#### Shape-Regularity

First of all, we define the *geometric vicinity* of an element  $T \in T_h$  by

$$\Delta(T) := \{ T' \in T_h \mid T \cap T' \neq \emptyset \}. \tag{23}$$

In the following, we will investigate the cardinality of the geometric vicinity and the volumes of its members, and for this purpose, we need to restrict ourselves to *shape-regular* meshes. Unfortunately, the definition of shape-regularity depends on the geometric shape of the elements  $T$  and various approaches have been proposed in the literature, see e.g. [6], [7], [10], [2] or [3]. Therefore, we exemplarily restrict ourselves to the two-dimensional case of shape-regular triangular meshes, where we provide geometrical arguments rather than formal proofs. We emphasise that the following arguments can be adapted to shape-regularity definitions of other element shapes and higher dimensions, as long as the shape-regularity prohibits ‘extreme’ cases such as e.g. quadrilateral elements degenerating to triangles.

**Definition 6:** Shape-Regularity by Zlámal [10]

A triangular mesh  $T_h$  is *shape-regular* if there exists a uniform constant  $\gamma > 0$ , such that for any triangle  $T \in T_h$  the inner angle of the two edges adjacent to any of the triangle's vertices is bounded below by  $\gamma$ .

As a direct result of this definition, we obtain a couple of properties:

a) For any vertex of the mesh the number of elements  $T \in T_h$  adjacent to that vertex is bounded above by  $\lfloor 2\pi/\gamma \rfloor$ . Furthermore, as any two different triangles  $T, T' \in T_h$  with  $T \cap T' \neq \emptyset$  share at least one common vertex for a conforming mesh and the fact that a triangle has three vertices, we directly obtain for all  $T \in T_h$  that

$$\text{card}(\Delta(T)) \leq M := 3\lfloor 2\pi/\gamma \rfloor. \quad (24)$$

b) If the basis  $B_h$  of our finite element space  $V_h$  is *local* in the sense that the support of any basis function  $\varphi_i \in B_h$ , which is associated with a single geometric entity<sup>1</sup>, is limited to all elements  $T \in T_h$  which are adjacent to that particular entity, then by (3) and (23) we directly obtain  $\delta(T) \subseteq \Delta(T)$  and (24) implies our assumption **(A3)** with  $c_3 = M$ .

c) Moreover, we can show by basic trigonometry<sup>2</sup> that for any two triangles  $T, T' \in T_h$ , which share a common edge, the areas of the two triangles are equivalent in the sense that

$$\varrho^{-1} \cdot \text{vol}(T') \leq \text{vol}(T) \leq \varrho \cdot \text{vol}(T') \quad (25)$$

for  $\varrho := \frac{1}{2\sin^3(\gamma)} > 1$ . Now consider two triangles  $T, T' \in T_h$ , which share a common vertex but no common edge. By the fact that our domain  $\Omega$  is assumed to have a Lipschitz boundary and that the mesh  $T_h$  is assumed to be conforming, we obtain that there exists a finite set of triangles  $\{T_1, \dots, T_m\} \subseteq \Delta(T)$ , such that  $T_1 = T$ ,  $T_m = T'$  and  $T_i$  shares a common edge with  $T_{i+1}$  for all  $1 \leq i < m$ . Combining this observation with (24) and (25), we obtain for any  $T \in T_h$  and any  $T' \in \Delta(T)$  that

$$\varrho^{-M} \cdot \text{vol}(T') \leq \text{vol}(T) \leq \varrho^M \cdot \text{vol}(T'), \quad (26)$$

which will be an important property for the verification of assumption **(A2)** later on.

## Parametric Finite Element Spaces

For the verification of our other assumptions, we first need to provide a definition of a parametric finite element space.

**Definition 7:** Parametric Finite Element Space

Let  $V_h$  denote a finite element space defined on a mesh  $T_h$  and let  $B_h = \{\varphi_1, \dots, \varphi_m\}$  denote the basis of  $V_h$ . We call  $V_h$  a *parametric space*, if there exists

1. a reference element  $\widehat{T} \subset \mathbb{R}^n$ ,
2. a reference basis  $\widehat{\varphi}_1, \dots, \widehat{\varphi}_l$  of a space  $\widehat{V}_h \subset \mathcal{L}^2(\widehat{T})$ ,

and for any  $T \in T_h$

3. a  $\mathcal{C}^1$ -diffeomorphism  $F_T : \widehat{T} \rightarrow T$ ,
4. a bijection  $j_T : \{1, \dots, l\} \rightarrow \mathcal{I}(T)$ ,

such that it holds for all  $1 \leq k \leq l$ :

$$\varphi_{j_T(k)}|_T \circ F_T = \widehat{\varphi}_k. \quad (27)$$

<sup>1</sup>A *geometric entity* may be a vertex, an edge, a face (in 3D) or an element.

<sup>2</sup>More precisely, by using the 'ASA rule' for triangle area computation.

Let us investigate the assumption **(BA)** for parametric finite element spaces: By construction of the discontinuous space  $\tilde{V}_h$  we have by (5) and (27) that

$$\tilde{\varphi}_{T,j_T(k)}|_T \circ F_T = \hat{\varphi}_k, \quad (28)$$

and 2., 3. and 4. of the previous definition directly imply that for any  $T \in T_h$  the functions  $\tilde{\varphi}_{T,i}|_T$  form a basis of  $\tilde{V}_h|_T = V_h|_T$ , which assures that the assumption **(BA)** holds.

**Lemma 8**

Let  $V_h$  denote a parametric finite element space defined on a conforming mesh  $T_h$ . If there exists a uniform constant  $c_J > 0$  such that for all  $T \in T_h$  the Jacobian determinant  $J_T : \hat{T} \rightarrow \mathbb{R}$  of  $F_T$  fulfills

$$\forall \hat{x} \in \hat{T} : c_J^{-1} \cdot \text{vol}(T) \leq J_T(\hat{x}) \leq c_J \cdot \text{vol}(T), \quad (29)$$

then the assumption **(A1)** holds for  $\tau_T = \sqrt{\text{vol}(T)}$ .

Before we continue with the proof of the lemma, let us investigate the new condition (29), which requires the Jacobian determinant  $J_T$  to be bounded against the volume of the element  $T$ . Note that the lemma does not directly require the mesh to be shape-regular, but in fact condition (29) is one of the basic estimates that are shown for shape-regular meshes. In [1, Theorem 4.3.3], Ciarlet provides an estimate for this condition in the case of *isoparametric* simplicial mappings and furthermore [7, Lemma 8] handles the case of bilinear quadrilateral mappings.

In the special case of shape-regular triangular meshes, which we have considered before, the mapping  $F_T$  is affine and its Jacobian determinant  $J_T$  therefore constant, so one can easily verify condition (29), where the constant  $c_J$  depends only on  $\gamma$  and other fixed quantities such as the volume of  $\hat{T}$ . Moreover, the result of the lemma combined with the estimate (26), which we have shown before, implies the last required assumption **(A2)** with  $c_2 = \varrho^{-M}$ .

We can now complete this section with the proof of the previous lemma.

*Proof of Lemma 8.* Let  $l := \dim(\hat{V}_h)$ , then the equivalence of norms on finite dimensional spaces implies that there exists a constant  $\hat{c} > 0$ , which only depends on  $\hat{T}$  and  $\hat{V}_h$ , such that for all  $x \in \mathbb{R}^l$

$$\hat{c}^{-1} \|x\|_2 \leq \left\| \sum_{k=1}^l x_k \cdot \hat{\varphi}_k \right\|_{0,\hat{T}} \leq \hat{c} \|x\|_2, \quad (*)$$

where  $\|\cdot\|_2$  denotes the euclidean norm on  $\mathbb{R}^l$  and  $\|\cdot\|_{0,\hat{T}}$  denotes the  $\mathcal{L}^2$  norm on  $\hat{T}$ .

Now let  $T \in T_h$  and  $\tilde{v}_h \in \tilde{V}_h$  be arbitrary and let  $\tilde{v}_{T,i} \in \mathbb{R}$  denote the coefficients of  $\tilde{v}_h$ . Then by (18) we have that

$$\|\tilde{v}_h\|_{0,T} = \|(\tilde{v}_{T,j_T(1)}, \dots, \tilde{v}_{T,j_T(l)})\|_2,$$

and combining this observation with (\*) and

$$\hat{v}_h := \tilde{v}_h \circ F_T = \sum_{k=1}^l \tilde{v}_{T,j_T(k)} \cdot (\tilde{\varphi}_{T,j_T(k)}^h|_T \circ F_T) \stackrel{(28)}{=} \sum_{k=1}^l \tilde{v}_{T,j_T(k)} \cdot \hat{\varphi}_k \quad (**)$$

directly leads us to the norm equivalence

$$\hat{c}^{-1} \|\tilde{v}_h\|_{0,T} \leq \|\hat{v}_h\|_{0,\hat{T}} \leq \hat{c} \|\tilde{v}_h\|_{0,T}. \quad (\dagger)$$

Furthermore, change of variables and (\*\*) lead to

$$\|\tilde{v}_h\|_{0,T}^2 = \int_T \tilde{v}_h(x)^2 dx = \int_{\hat{T}} |J_T(\hat{x})| \cdot \hat{v}_h(\hat{x})^2 d\hat{x}, \quad (\ddagger)$$

and the upper bound of (29) yields

$$\|\tilde{v}_h\|_{0,T}^2 \stackrel{(\ddagger)}{\leq} c_J \cdot \text{vol}(T) \cdot \|\hat{v}_h\|_{0,\hat{T}}^2 \stackrel{(\dagger)}{\leq} c_J \cdot \text{vol}(T) \cdot \hat{c}^2 \cdot \|\tilde{v}_h\|_{0,T}^2. \quad (\S)$$

Analogously, we have that

$$\|\tilde{v}_h\|_{0,T}^2 \stackrel{(\dagger)}{\leq} \hat{c}^2 \cdot \|\hat{v}_h\|_{0,\hat{T}}^2 = \hat{c}^2 \int_{\hat{T}} \hat{v}_h(\hat{x})^2 d\hat{x} = \hat{c}^2 \int_T |J_T^{-1}(x)| \cdot \tilde{v}_h(x)^2 dx. \quad (\ddagger\ddagger)$$

The inverse function theorem yields

$$\sup_{x \in T} |J_T^{-1}(x)| = \sup_{\hat{x} \in \hat{T}} |(J_T(\hat{x}))^{-1}| = \left( \inf_{\hat{x} \in \hat{T}} |J_T(\hat{x})| \right)^{-1},$$

and with the lower bound of (29) we obtain

$$\|\tilde{v}_h\|_{0,T}^2 \stackrel{(\ddagger\ddagger)}{\leq} c_J \cdot \text{vol}(T)^{-1} \cdot \hat{c}^2 \cdot \|\tilde{v}_h\|_{0,T}^2,$$

which together with  $(\dagger)$  proves **(A1)** for  $\tau_T := \sqrt{\text{vol}(T)}$  and  $c_1 = \sqrt{c_J} \cdot \hat{c}$ . ■

## 5 Practical aspects

We now focus on the implementational aspects of our projection operator. In particular, we want to consider two scenarios:

1. The projection of an arbitrary function  $u \in \mathcal{L}^2(\Omega)$  into a finite element space  $V_h \subset \mathcal{L}^2(\Omega)$ .
2. The projection of a discrete function  $u_h^{(1)}$  of one finite element space  $V_h^{(1)}$  into another finite element space  $V_h^{(2)}$  – possibly defined on a different mesh.

Obviously, the latter case is a special case of the former one, however, for this scenario we will assemble our projection operator into a sparse matrix, such that any  $u_h^{(1)} \in V_h^{(1)}$  can be projected into  $V_h^{(2)}$  by simply performing a matrix-vector multiplication with the coefficient vector of  $u_h^{(1)}$ .

Both operations can be implemented as modified versions of standard assembly operations, utilising only software components which are already required for the assembly of a right hand side vector and a mass matrix. We will not go into technical details of the standard assembly process and we refer the interested reader to [11, Section 3] or [12, Section 4] for more information.

### 5.1 Projections of arbitrary functions

In the following, let  $u \in \mathcal{L}^2(\Omega)$  be an arbitrary function and let  $B_h = \{\varphi_1, \dots, \varphi_m\}$  denote a basis of a finite element space  $V_h$  defined on a mesh  $T_h$ . For any  $T \in T_h$  let  $l_T := \text{card}(\mathcal{I}(T))$  and let  $j_T : \{1, \dots, l_T\} \rightarrow \mathcal{I}(T)$  denote a bijection as in Definition 7. Within the algorithms, we omit the subscript  $T$  and write  $l$  and  $j$  instead of  $l_T$  and  $j_T$  for better readability.

The following algorithm describes the steps required assemble the coefficient vector  $\mathbf{u} \in \mathbb{R}^m$  of the projection  $u_h := P_h^\omega(u)$ .

#### Algorithm 1: Projection Assembly

1. Allocate the vector  $\mathbf{u} \in \mathbb{R}^m$ , a weight vector  $\mathbf{w} \in \mathbb{R}^m$  and initialise their entries to zero.
2. For each  $T \in T_h$  with  $j : \{1, \dots, l\} \rightarrow \mathcal{I}(T)$  do:
  - (a) Assemble the local right-hand-side vector  $\mathbf{u}_T^* \in \mathbb{R}^l$ ,  
i.e. for all  $1 \leq i \leq l$  compute

$$\mathbf{u}_{T,i}^* \leftarrow \int_T u \cdot \varphi_{j(i)} dx.$$

- (b) Assemble the local mass matrix  $\mathbf{M}_T \in \mathbb{R}^{l \times l}$ ,  
i.e. for all  $1 \leq i, k \leq l$  compute

$$\mathbf{M}_{T,i,k} \leftarrow \int_T \varphi_{j(i)} \cdot \varphi_{j(k)} dx.$$

- (c) Compute the solution  $\mathbf{u}_T \in \mathbb{R}^l$  of the local system  $\mathbf{M}_T \cdot \mathbf{u}_T = \mathbf{u}_T^*$ .
- (d) Choose a local weight vector  $\mathbf{w}_T \in \mathbb{R}^l$  with non-negative entries.
- (e) Incorporate the local vector  $\mathbf{u}_T$  into  $\mathbf{u}$  by a weighted scatter-add operation, i.e. for all  $1 \leq i \leq l$  update

$$\mathbf{u}_{j(i)} \leftarrow \mathbf{u}_{j(i)} + \mathbf{w}_{T,i} \cdot \mathbf{u}_{T,i}.$$

- (f) Incorporate the local weight vector  $\mathbf{w}_T$  into  $\mathbf{w}$  by a scatter-add operation, i.e. for all  $1 \leq i \leq l$  update

$$\mathbf{w}_{j(i)} \leftarrow \mathbf{w}_{j(i)} + \mathbf{w}_{T,i}.$$

3. Scale the vector  $\mathbf{u}$  by the reciprocals of the weights, i.e. for all  $1 \leq i \leq m$  update:

$$\mathbf{u}_i \leftarrow \mathbf{u}_i / \mathbf{w}_i.$$

In section (3) we have proposed two possible choices of the weights  $\omega_{T,i} \in \mathbb{R}$  and we now want to show how the local weight vectors  $\mathbf{w}_T$  have to be chosen to obtain these weights  $\omega_{T,i}$ . The first choice, namely the *arithmetic average*, is obtained by choosing

$$\forall T \in T_h : \mathbf{w}_T \equiv 1 \quad \implies \quad \omega_{T,i} = \frac{1}{\text{card}(\sigma(i))},$$

and the *volume-weighted average* is obtained by

$$\forall T \in T_h : \mathbf{w}_T \equiv \text{vol}(T) \quad \implies \quad \omega_{T,i} = \frac{\text{vol}(T)}{\text{vol}(\sigma(i))}.$$

As assembling the local mass matrix  $\mathbf{M}_T$  already requires the usage of a cubature rule on each element  $T \in T_h$ , one can also use this cubature rule to compute the volume of  $T$  at no additional cost.

## 5.2 Projections between Finite Element spaces

Let  $B_h^{(1)} = \{\varphi_1^{(1)}, \dots, \varphi_m^{(1)}\}$  and  $B_h^{(2)} = \{\varphi_1^{(2)}, \dots, \varphi_n^{(2)}\}$  denote the bases of two finite element spaces  $V_h^{(1)}$  and  $V_h^{(2)}$  defined on a mesh  $T_h$ . We now want to derive an assembly for our projection operator  $P_h^\omega : \mathcal{L}^2(\Omega) \supset V_h^{(1)} \rightarrow V_h^{(2)}$  from the previous assembly Alg. 1 we have presented for the projections of arbitrary functions. The first important observation is that any  $u_h^{(1)} \in V_h^{(1)}$  is uniquely determined by its coefficient vector  $\mathbf{u}^{(1)} \in \mathbb{R}^m$ , which allows us to replace the local assembly of  $\mathbf{u}_T^*$  in step (2.a) of Alg. 1 by the assembly of a local *inter-space mass matrix*  $\mathbf{N}_T$ , which uses  $V_h^{(1)}$  as the *ansatz space* and  $V_h^{(2)}$  as the *test space*. In consequence, we assemble a projection matrix  $\mathbf{P} \in \mathbb{R}^{m \times n}$ , such that  $\mathbf{u}^{(2)} := \mathbf{P} \cdot \mathbf{u}^{(1)}$  denotes the coefficient vector of  $u_h^{(2)} := P_h^\omega(u_h^{(1)})$ , where  $\mathbf{u}^{(1)} \in \mathbb{R}^m$  is the coefficient vector of some  $u_h^{(1)} \in V_h^{(1)}$ . As our projection operator only performs element-wise  $\mathcal{L}^2$ -projections by construction, the matrix  $\mathbf{P}$  has the same sparsity pattern as the global inter-space mass matrix  $\mathbf{N} \in \mathbb{R}^{m \times n}$ , which can be pre-computed before assembling the actual matrix, see e.g. [16].

**Algorithm 2:** Projection Matrix Assembly

1. Allocate the projection matrix  $\mathbf{P} \in \mathbb{R}^{m \times n}$ , a weight vector  $\mathbf{w} \in \mathbb{R}^m$  and initialise their entries to zero.
2. For each  $T \in T_h$  with  $j^{(1)} : \{1, \dots, l\} \rightarrow \mathcal{I}^{(1)}(T)$  and  $j^{(2)} : \{1, \dots, r\} \rightarrow \mathcal{I}^{(2)}(T)$  do:
  - (a) Assemble the local inter-space mass matrix  $\mathbf{N}_T \in \mathbb{R}^{l \times r}$ , i.e. for all  $1 \leq i \leq l$  and all  $1 \leq k \leq r$  compute

$$\mathbf{N}_{T,i,k} \leftarrow \int_T \varphi_{j^{(2)}(i)}^{(2)} \cdot \varphi_{j^{(1)}(k)}^{(1)} dx.$$

- (b) Assemble the local target space mass matrix  $\mathbf{M}_T \in \mathbb{R}^{l \times l}$ ,  
i.e. for all  $1 \leq i, k \leq l$  compute

$$\mathbf{M}_{T,i,k} \leftarrow \int_T \varphi_{j^{(2)}(i)}^{(2)} \cdot \varphi_{j^{(2)}(k)}^{(2)} dx.$$

- (c) Compute the solution  $\mathbf{P}_T \in \mathbb{R}^{l \times r}$  of the local system  $\mathbf{M}_T \cdot \mathbf{P}_T = \mathbf{N}_T$ .  
(d) Choose a local weight vector  $\mathbf{w}_T \in \mathbb{R}^l$  with non-negative entries.  
(e) Incorporate the local matrix  $\mathbf{P}_T$  into  $\mathbf{P}$  by a weighted scatter-add operation,  
i.e. for all  $1 \leq i \leq l$  and all  $1 \leq k \leq r$  update

$$\mathbf{P}_{j^{(2)}(i),j^{(1)}(k)} \leftarrow \mathbf{P}_{j^{(2)}(i),j^{(1)}(k)} + \mathbf{w}_{T,i} \cdot \mathbf{P}_{T,i,k}.$$

- (f) Incorporate the local weight vector  $\mathbf{w}_T$  into  $\mathbf{w}$  by a scatter-add operation,  
i.e. for all  $1 \leq i \leq l$  update

$$\mathbf{w}_{j^{(2)}(i)} \leftarrow \mathbf{w}_{j^{(2)}(i)} + \mathbf{w}_{T,i}.$$

3. Scale the rows of  $\mathbf{P}$  by the reciprocals of the weights,  
i.e. for all  $1 \leq i \leq m$  and  $1 \leq k \leq n$  update:

$$\mathbf{P}_{i,k} \leftarrow \mathbf{P}_{i,k} / \mathbf{w}_i.$$

### 5.2.1 Prolongation Matrices for Geometric Multigrid Methods

One of the main applications of our projection operator is its usage as a prolongation and restriction operator for geometric multigrid methods, see e.g. [4]. Assume that a mesh  $T_h$  has been created by some sort of refinement of another mesh  $T_{2h}$  and let  $V_h^{(1)}$  denote the coarse mesh space defined on  $T_{2h}$  and let  $V_h^{(2)}$  denote the fine mesh space defined on  $T_h$ . Under the assumption that the two meshes  $T_h$  and  $T_{2h}$  are *nested*, i.e.  $\forall T \in T_h : \exists T' \in T_{2h} : T \subseteq T'$ , then the assembly algorithm for the projection operator  $P_h^\omega : V_h^{(1)} \rightarrow V_h^{(2)}$  is identical to the one proposed in Alg. 2, with the modification that for each  $T \in T_h$  one first has to determine the corresponding parent element  $T' \in T_{2h}$ , such that  $T \subseteq T'$ , and consider the mapping  $j^{(2)} : \{1, \dots, r\} \rightarrow \mathcal{I}^{(2)}(T')$  instead.

The practical challenge is the assembly of the local inter-space mass matrix  $\mathbf{N}_T$  in step (2.a): The integral is usually approximated by a cubature formula, which requires that the cubature points are mapped onto the corresponding parent element  $T' \in T_{2h}$  to evaluate the basis functions of  $V_h^{(1)}$ . However, this problem is not specific to our projection operator, but arises for any type of assembly with test and ansatz spaces defined on different meshes. In consequence, if a finite element software package is capable of assembling an inter-space mass matrix for test and ansatz spaces on different meshes, then the corresponding assembly method can easily be modified to obtain the assembly method for our projection operator as proposed in Alg. 2.

### 5.2.2 Post-Processing of the Projection Matrix

In the case of *nested* finite element spaces, i.e. where  $V_h^{(1)} \subseteq V_h^{(2)}$ , the projection matrix  $\mathbf{P}$  will often have much less non-zero entries than the corresponding inter-space matrix sparsity pattern. Therefore, one may think about the possibility of *filtering* the projection matrix  $\mathbf{P}$  after its assembly, i.e., removing all ‘non-zeroes’ whose absolute value is below a tolerance parameter close to machine precision, thus reducing memory consumption and avoiding redundant multiplications with zeroes when applying the projection.

Consider the case where  $V_h^{(1)}$  is the  $Q_1$  finite element space defined on a 3D structured  $n \times n \times n$  tensor-product mesh  $T_{2h}$ , and  $V_h^{(2)}$  is the  $Q_1$  space on the corresponding refined  $2n \times 2n \times 2n$  tensor-product mesh  $T_h$ , then the standard inter-space matrix sparsity pattern has  $125n^3 + \mathcal{O}(n^2)$  entries, whereas the projection matrix  $\mathbf{P}$  contains only  $27n^3 + \mathcal{O}(n^2)$  actual non-zero entries – therefore filtering the projection matrix reduces its size by (asymptotically) 78,4%.

## 6 Numerical Experiments

In this section, we perform a set of numerical experiments to analyse our new projection operator  $P_h^\omega$ , where we use the *volume-weighted average* as given in (15) for its definition. We compare the projection  $\mathcal{L}^2$ -errors with those of the standard interpolation operator  $\Pi_h$  as well as the  $\mathcal{L}^2$ -projection, which we shall denote as  $P_h^*$ . We investigate four different triangular elements: The  $\mathcal{H}^1$ -conforming first- and second-order Lagrange  $P_1$  and  $P_2$  elements, the  $\mathcal{H}^2$ -conforming quintic Argyris (*Ar*) element, see e.g. [1], as well as the nonconforming first-order Crouzeix-Raviart (*CR*) element, see [8]. All our experiments are performed on the domain  $\Omega := (-1, 1)^2 \subset \mathbb{R}^2$ . The mesh sequence we use for our experiments is generated by successively refining a coarse mesh. The coarse mesh consists of eight triangles, which emerge from ‘cutting’ the domain  $\Omega$  along all lines connecting two edge midpoints, see Fig. 1a. The refinement procedure subdivides each parent triangle into four children along the edges that emerge from connecting the parent triangle’s edge midpoints, see Fig. 1b. Moreover, we ‘emulate’ a grid deformation process for the second experiment by replacing each vertex coordinate  $v_i$  of the refined mesh using the formula

$$v'_i := \sin(\pi v_i/2),$$

which results in a mesh with smaller but more anisotropic elements near the boundary, see Fig. 1c.

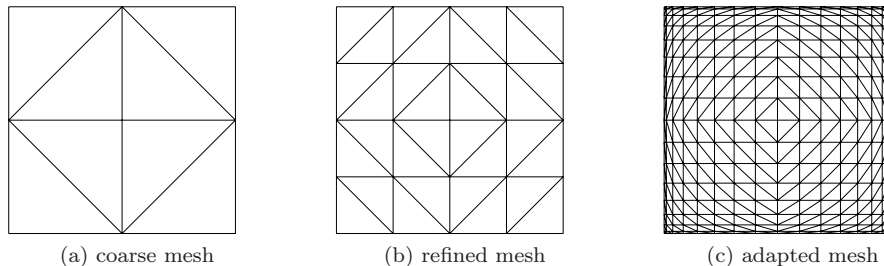


Figure 1: Left: The level 1 (coarse) mesh. Middle: The level 2 (refined) mesh. Right: The level 4 adapted mesh.

### 6.1 Cosine-Bubble Function

The first experiment is the projection of the cosine-bubble function

$$u(x, y) = \cos(\pi x/2) \cos(\pi y/2).$$

Table 1 summarises the  $\mathcal{L}^2$ -errors of the standard interpolation operator  $\Pi_h$ , our projection operator  $P_h^\omega$  and the  $\mathcal{L}^2$ -projection  $P_h^*$  for the  $P_1$ ,  $P_2$ , Crouzeix-Raviart and Argyris elements for the first six non-adapted mesh refinement levels. All three projection techniques yield the full approximation order for all four tested elements, where the errors of our new projection operator are almost identical to the errors of the full  $\mathcal{L}^2$  projection.

### 6.2 Exponential Function

For the second experiment, we consider the function

$$u(x, y) = \frac{(e^{10} - e^{10x^2}) \cdot (e^{10} - e^{10y^2})}{(e^{10} - 1)^2}.$$

As the function has steep gradients at the domain boundary, we perform this experiment on the adapted mesh sequence. Note that the adapted mesh sequence violates the shape regularity condition from Definition 6 as the minimal inner angle tends to zero for triangles at the domain boundary. In consequence, our a-priori estimates are not applicable for this numerical experiment. However, Table 2 shows that even in this case the errors of our projection operator  $P_h^\omega$  are only slightly greater than the errors of the full  $\mathcal{L}^2$ -projection operator  $P_h^*$ .

Level	$P_1 : \Pi_h$	$P_1 : P_h^\omega$	$P_1 : P_h^*$	$P_2 : \Pi_h$	$P_2 : P_h^\omega$	$P_2 : P_h^*$
2	1.417E-01	6.271E-02	6.020E-02	6.459E-03	3.943E-03	3.858E-03
3	3.601E-02	1.528E-02	1.504E-02	8.610E-04	6.522E-04	6.335E-04
4	9.042E-03	3.730E-03	3.717E-03	1.092E-04	9.563E-05	9.362E-05
5	2.263E-03	9.262E-04	9.256E-04	1.370E-05	1.286E-05	1.272E-05
6	5.659E-04	2.312E-04	2.312E-04	1.714E-06	1.662E-06	1.653E-06
7	1.415E-04	5.777E-05	5.777E-05	2.143E-07	2.110E-07	2.105E-07
Level	$CR : \Pi_h$	$CR : P_h^\omega$	$CR : P_h^*$	$Ar : \Pi_h$	$Ar : P_h^\omega$	$Ar : P_h^*$
2	7.307E-02	4.640E-02	4.640E-02	1.033E-04	6.923E-05	1.619E-05
3	1.814E-02	1.151E-02	1.151E-02	1.614E-06	1.106E-06	2.313E-07
4	4.530E-03	2.868E-03	2.868E-03	2.523E-08	1.905E-08	3.442E-09
5	1.132E-03	7.163E-04	7.163E-04	3.943E-10	3.172E-10	5.249E-11
6	2.830E-04	1.790E-04	1.790E-04	6.161E-12	5.101E-12	8.106E-13
7	7.075E-05	4.475E-05	4.475E-05	9.625E-14	3.397E-13	1.276E-14

Table 1:  $\mathcal{L}^2$ -Errors for the cosine-bubble function.

Level	$P_1 : \Pi_h$	$P_1 : P_h^\omega$	$P_1 : P_h^*$	$P_2 : \Pi_h$	$P_2 : P_h^\omega$	$P_2 : P_h^*$
2	5.680E-01	2.191E-01	2.154E-01	1.733E-01	9.476E-02	8.834E-02
3	1.259E-01	5.060E-02	4.984E-02	2.180E-02	1.658E-02	1.558E-02
4	4.189E-02	1.856E-02	1.805E-02	3.685E-03	3.271E-03	3.140E-03
5	1.074E-02	4.347E-03	4.321E-03	4.742E-04	4.572E-04	4.495E-04
6	2.704E-03	1.069E-03	1.068E-03	5.971E-05	5.905E-05	5.872E-05
7	6.772E-04	2.663E-04	2.663E-04	7.477E-06	7.450E-06	7.437E-06
Level	$CR : \Pi_h$	$CR : P_h^\omega$	$CR : P_h^*$	$Ar : \Pi_h$	$Ar : P_h^\omega$	$Ar : P_h^*$
2	2.992E-01	1.680E-01	1.680E-01	8.673E-02	1.666E-01	3.987E-03
3	6.060E-02	3.841E-02	3.841E-02	3.940E-03	4.577E-03	3.307E-04
4	2.010E-02	1.341E-02	1.341E-02	5.966E-05	6.581E-05	5.229E-06
5	5.129E-03	3.358E-03	3.358E-03	9.513E-07	1.075E-06	7.950E-08
6	1.290E-03	8.384E-04	8.384E-04	1.495E-08	1.757E-08	1.237E-09
7	3.230E-04	2.094E-04	2.094E-04	2.340E-10	2.788E-10	1.932E-11

Table 2:  $\mathcal{L}^2$ -Errors for the exponential function.

## 7 Conclusions

In this work, we have shown how the  $\mathcal{L}^2$ -projection operator can be approximated by a set of element-wise  $\mathcal{L}^2$ -projections in combination with a weighted restriction operator. The resulting operator can be realised as a modified standard assembly algorithm, which proves to be a benefit over other interpolation operators utilising the finite element spaces node functionals, as it can be implemented as a ‘black-box’ method. Moreover, the fact, that our projection operator can be directly assembled as a sparse matrix for projections between two finite element spaces, makes it an ideal candidate for use as a prolongation and restriction operator in geometric multigrid methods.

Our theoretical analysis revealed that under a small set of abstract assumptions, which can be verified for a large set of finite elements, the  $\mathcal{L}^2$ -error of our projection operator is bounded by the discretisation error, which we have verified in numerical examples in two dimensions.

## Acknowledgements

This work was supported (in part) by the German Research Foundation (DFG) through the Priority Programme 1648 ‘‘Software for Exascale Computing’’ (SPPEXA): projects TU 102/48-1 and GO 1758/2-1.

## References

- [1] P.G. CIARLET: *The Finite Element Method for Elliptic Problems*; 2nd edition, SIAM, 2002, ISBN: 978-0-89871-514-9
- [2] S.C. BRENNER, L.R. SCOTT: *The Mathematical Theory of Finite Element Methods*; 3rd edition, Springer, 2008, ISBN: 978-0-387-75933-3
- [3] D. BRAESS: *Finite Elements: Theory, fast solvers, and applications in solid mechanics*; 3rd edition, Cambridge University Press, 2007, ISBN: 978-0-521-70518-9
- [4] W. HACKBUSCH: *Multi-Grid Methods and Applications*; 2nd edition, Springer, 2003, ISBN: 978-3-540-12761-1
- [5] PH. CLÉMENT: *Approximation by finite element functions using local regularization*; RAIRO Analyse Numérique, Volume 9, Issue 2 (1975), pp. 77–84
- [6] P.G. CIARLET, P.-A. RAVIART: *General Lagrange and Hermite Interpolation in  $R^n$  with Applications to Finite Element Methods*; Archive for Rational Mechanics and Analysis, Volume 46, Issue 3 (1972), pp. 177–199
- [7] P.G. CIARLET, P.-A. RAVIART: *Interpolation theory over curved elements with applications to finite element methods*; Computer Methods in applied Mechanics and Engineering, Volume 1 (1972), pp. 217–249
- [8] M. CROUZEIX, P.-A. RAVIART: *Conforming and Nonconforming Finite Element methods for solving the stationary Stokes equations I*; RAIRO, Volume 7, Number 3 (1973), pp. 33–76
- [9] R. RANNACHER, S. TUREK: *Simple Nonconforming Quadrilateral Stokes Element*; Numerical Methods for Partial Differential Equations, Volume 8, Issue 2 (1992), pp. 97–111
- [10] M. ZLÁMAL: *On the Finite Element Method*; Numerische Mathematik, Volume 12, Issue 5 (1968), pp. 394–409
- [11] A. LOGG: *Automating the Finite Element Method*; Archives of Computational Methods in Engineering, Volume 14, Issue 2 (2007), pp. 93–138
- [12] G.R. MARKALL, A. SLEMMER, D.A. HAM, P.H.J. KELLY, C.D. CANTWELL, S.J. SHERWIN: *Finite element assembly strategies on multi-core and many-core architectures*; International Journal for Numerical Methods in Fluids, Volume 71, Issue 1 (2013), pp. 80–97
- [13] L.R. SCOTT, S. ZHANG: *Finite Element Interpolation of Nonsmooth Functions Satisfying Boundary Conditions*; Mathematics of Computation, Volume 54, Number 190 (1990), pp. 483–493
- [14] Y. JEON, H. NAM, D. SHEEN: *A nonconforming quadrilateral element with maximal inf-sup constant*; Numerical Methods for Partial Differential Equations, Volume 30, Issue 1 (2014), pp. 120–132
- [15] F. SCHIEWECK: *A General Transfer Operator for Arbitrary Finite Element Spaces*; Preprint Nr. 25/00, Fakultät für Mathematik, Universität Magdeburg, 2000
- [16] P. ZAJAC: *Assembling Adjacency Relations for the Finite Element Method*; Ergebnisberichte des Instituts für Angewandte Mathematik, Nummer 476, Fakultät für Mathematik, TU Dortmund, 2013